Inorganic Chemistry

Article

pubs.acs.org/IC

Single-Molecule Magnet of a Tetranuclear Dysprosium Complex Disturbed by a Salen-Type Ligand and Chloride Counterions

Fang Luan,[†,‡] Tianqi Liu,[†] Pengfei Yan,[†] Xiaoyan Zou,[†] Yuxin Li,[†] and Guangming Li*[,†]

[†]Key Laboratory of Functional Inorganic Material Chemistry, School of Chemistry and Materials Science, Heilongjiang University, Harbin 150080, P. R. China

[‡]School of Pharmacy, Jiamusi University, Jiamusi 154007, P. R. China

Supporting Information

ABSTRACT: A series of three salen-type lanthanide complexes, e.g., $[Dy_4(L)_2(HL)_2Cl_2(\mu_3\text{-}OH)_2]_2Cl_2(OH)_2\cdot 3CH_3CH_2OH\cdot H_2O$ (**1**) and $[Ln_4(L)_2(HL)_2Cl_2(\mu_3\text{-}OH)_2]Cl_2\cdot 5CH_3OH\cdot 4CH_2Cl_2$ (Ln = Tb^{III}, **2**; Ho^{III}, **3**) have been isolated by the reactions of H_2L (H_2L = *N*,*N*′-bis(3-methoxysalicylidene)cyclohexane-1,2-diamine) with $LnCl_3\cdot 6H_2O$. X-ray crystallographic analysis reveals that all complexes **1**−**3** are isostructural, in which four Ln ions and eight O atoms form the distorted defective dicubane $\{Dy_4O_8\}$ cores. Magnetic studies indicate that complex **1** exhibits two slow magnetic relaxation processes with effective energy barrier U_{eff} = 55.71 K under a zero direct-current field, which is attributed to the two coordination geometries of the Dy^{III} ions with a salen-type ligand and coordination of a chloride counterion. It represents the highest energy barrier among the salen-type tetranuclear lanthanide single-molecule magnets.

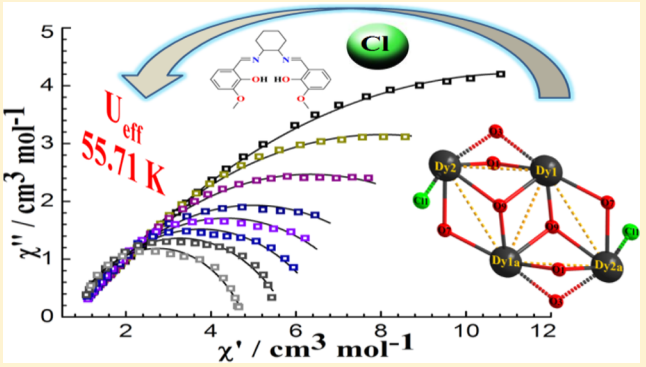

INTRODUCTION

Single-molecule magnets (SMMs) continue to attract considerable attention of both physicists and chemists because of their potential applications in high-density information storage[1] and molecule-based spintronic devices.[2] In recent years, a variety of transition-metal,[3] lanthanide,[4] and 3d−4f[5] SMMs have been synthesized as molecule counterparts to magnetic nanoparticles. One of the most promising ways to obtain high-energy-barrier SMMs is by way of Ln ions because of their large intrinsic magnetic anisotropy arising from their large unquenched orbital angular momentum.[6] In 2003,[7] Ishikawa et al. reported the first Ln-ion-based SMMs, which opened a new page in modern magnetic material chemistry. However, among the lanthanide family, the Dy^{III} ion attributed to the inherently large magnetic moment with a Kramers ground state of $^6H_{15/2}$, and a large Ising-type magnetic anisotropy has indisputably led to the largest number of pure 4f SMMs.[8] To date, various SMMs of mononuclear,[9] dinuclear,[10] trinuclear,[11] tetranuclear,[12] and polynuclear[13] dysprosium complexes have been reported in which the largest effective energy barrier of a dysprosium SMM was 528 K.[14] However, pure 4f-based polynuclear SMMs are relatively scarce because of the difficulty in promoting magnetic interactions between the bridging ligand orbital and the 4f orbital of the Ln ions. It is known that the ligand field is one of the most important factors for constructing 4f SMMs.[15] Among the numerous ligands, e.g., salen-type ligands, β-diketonate ligands, and carboxylic acid and its derivative ligands, the salen-type ligands have been proven to be particularly suitable for the synthesis of 4f SMMs, such as 1D chain,[16] dinuclear,[16,17] trinuclear,[18] and tetranuclear,[17g,19] while it is worth noting that the energy barrier of the reported pure salen-type SMMs are not high enough, in which the highest energy barrier is 101 K for the dinuclear complex $[Dy_2(L^2)_4](H_2O)(DMF)_{0.5}$ synthesized by the ligand *N*,*N*′-bis(3-methoxysalicylidene)biphenyl-4,4′-diamine[17c] and only 17.2 K for pure salen-type tetranuclear SMMs.[19a]

In order to enhance the energy barrier of polynuclear salen-type SMMs and explore the effect of counterions, we selected the semirigid hexadentate salen-type ligand of *N*,*N*′-bis(3-methoxysalicylidene)cyclohexane-1,2-diamine and $LnCl_3\cdot 6H_2O$ to construct the SMMs of salen-type lanthanide complexes. As a result, a series of three salen-type tetranuclear lanthanide complexes have been isolated. Their crystal structures have been determined and their static and dynamic magnetic properties studied.

EXPERIMENTAL SECTION

Materials and Instrumentation. Solvents and other general reagents used for this work except $LnCl_3\cdot 6H_2O$ and *N*,*N*′-bis(3-methoxysalicylidene)cyclohexane-1,2-diamine (H_2L) were commercial products of reagent grade and were used without further purification. All manipulations were performed under ambient/aerobic conditions. H_2L was synthesized according to literature procedures.[20] Elemental

Received: January 9, 2015
Published: March 23, 2015

DOI: 10.1021/acs.inorgchem.5b00061
Inorg. Chem. 2015, 54, 3485−3490

Table 1. Crystal Data and Structure Refinement for Complexes 1−3

	1	2	3
CCDC	1024672	1024673	1024674
formula	$C_{182}H_{218}Cl_6Dy_8N_{16}O_{42}$	$C_{98}H_{120}Cl_{12}Tb_4N_8O_{24}$	$C_{98}H_{120}Cl_{12}Ho_4N_8O_{24}$
fw	4814.44	2855.15	2879.15
cryst color	yellow	yellow	yellow
cryst syst	monoclinic	monoclinic	monoclinic
space group	$P2_1/c$	$P2_1/c$	$P2_1/c$
a (Å)	18.4659(5)	17.8721(4)	17.8921(5)
b (Å)	16.3855(4)	16.5942(4)	16.5528(4)
c (Å)	25.4416(7)	24.4103(6)	24.4805(6)
α (deg)	90	90	90
β (deg)	132.218(2)	130.183(1)	130.332(2)
γ (deg)	90	90	90
V (Å^3)	5701.0(3)	5530.8(2)	5526.9(3)
Z	1	2	2
D_{calcd} (mg/cm^3)	1.402	1.714	1.730
μ (mm^{-1})	2.722	2.888	3.194
F(000)	2388.0	2840.0	2856.0
θ range (deg)	2.90−25.00	3.23−25.00	2.92−25.00
R1 [$I > 2\sigma(I)$]	0.0508	0.0476	0.0526
wR2 [$I > 2\sigma(I)$]	0.1296	0.1176	0.1307
R1 (all data)	0.0876	0.0676	0.0762
wR2 (all data)	0.1467	0.1332	0.1495
GOF on F^2	1.083	0.994	1.062

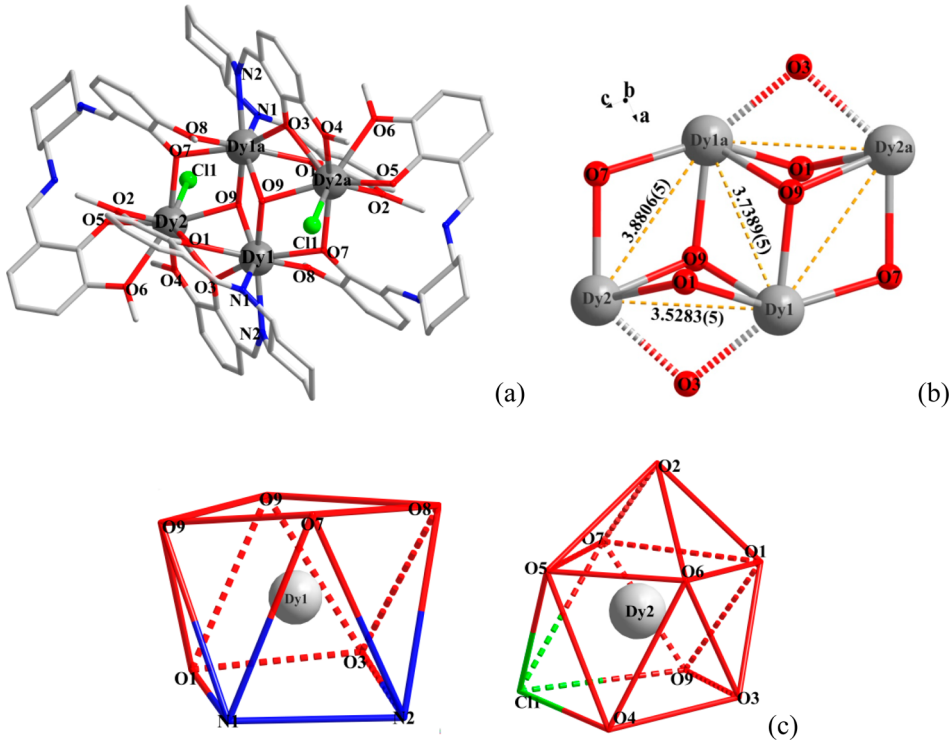

Figure 1. (a) Molecular structure of the cationic part for complex **1**. H atoms and solvates are omitted for clarity. (b) Distorted defective dicubane $\{Dy_4O_8\}$ core consisting of two edge-shared triangular dimeric $[Dy_3(OH)]^{8+}$ subunits. (c) Two coordination geometries of Dy1 and Dy2 ions.

analyses were performed for C, H, and N on a Perkin-Elmer 2400 analyzer. UV spectra data were collected on a Perkin-Elmer 35 spectrophotometer. Fourier transform infrared (FT-IR) spectral data were recorded on a Perkin-Elmer 100 spectrophotometer using KBr pellets from 4000 to 500 cm^{-1}. Powder X-ray diffraction (PXRD) data were selected on a Rigaku D/Max-3B X-ray diffractometer with Cu Kα as the radiation source (λ = 0.15406 nm) in the angular range θ = 5−50° at room temperature. Thermal analyses were carried out on a STA-6000 analyzer with a heating rate of 10 °C min^{-1} in the range of 30−800 °C under a N_2 atmosphere. The magnetic susceptibilities of complexes **1**−**3** (polycrystalline samples) were carried out with a Quantum Design SQUID MPMS-XL7 magnetometer.

Synthesis of $[Dy_4L_2(HL)_2Cl_2(\mu_3\text{-}OH)_2]_2Cl_2(OH)_2\cdot 3CH_3CH_2OH\cdot H_2O$ (1). H_2L (0.25 mmol, 96 mg) was dissolved in EtOH (15 mL) in the presence of triethylamine (0.6 mmol, 84 μL), and then $DyCl_3\cdot 6H_2O$ (0.25 mmol, 94 mg) was added under stirring. The yellow

DOI: 10.1021/acs.inorgchem.5b00061
Inorg. Chem. 2015, 54, 3485−3490

Table 2. Differences of the Structural and Magnetic Parameters among Complex 1 and the Reported Salen-Type Dy_4 SMMs

complex	coordination mode	Ln_4 core	symmetry point group	U_{eff} value (K)	ref
1 [H_2L = *N*,*N*′-bis(3-methoxysalicylidene)cyclohexane-1,2-diamine]	O_8Cl, N_2O_6	$\{Dy_4O_8\}$	C_{4v}, C_{2v}	55.71	
$[Dy_4L_2(HL)_2(NO_3)_2(\mu_3\text{-}OH)_2]$ [H_2L = *N*,*N*′-bis(3-methoxysalicylidene)cyclohexane-1,2-diamine]	O_9, N_2O_6	$\{Dy_4O_8\}$	C_{4v}, C_{2v}	48.14	19d
$[Dy_4(\mu_3\text{-}OH)_2L_2(acac)_6]$ [H_2L = *N*,*N*′-bis(salicylidene)-1,2-cyclohexanediamine]	O_8, N_2O_6	$\{Dy_4O_8\}$	D_{4d}	22 (1400 Oe)	15b
$[Dy_4(\mu_3\text{-}OH)_2L^2{}_2(acac)_6]$ [H_2L = *N*,*N*′-bis(salicylidene)-1,2-ethanediamine]	O_8, N_2O_6	$\{Dy_4O_8\}$	D_{4d}	13.95	15b
$[Dy_4(\mu_4\text{-}O)L_2(C_6H_5COO)_6]$ [H_2L = *N*,*N*′-bis(3-methoxysalicylidene)cyclohexane-1,2-diamine]	O_8, N_2O_6	$\{Dy_4O_7\}$	C_{2v}	2.3	13d
$[Dy_4(salen)_6]$ [H_2L = *N*,*N*′-ethylenebis(salicylideneiminato) dianion]	N_4O_4, N_2O_5	$\{Dy_4O_6\}$	C_{2v}, D_{2d}	17.2	15a

solution was stirred for 24 h and then filtered. Diethyl ether was allowed to diffuse slowly into the filtrate at ambient temperature. Yellow rhombic-shaped crystals were obtained after 2 weeks. Yield: 63 mg (42%). Elem anal. Calcd for $C_{182}H_{218}Cl_6Dy_8N_{16}O_{42}$ (4814.44): C, 45.40; H, 4.56; N, 4.65. Found: C, 45.30; H, 4.54; N, 4.71. IR (KBr, cm^{-1}): 3404, 2930, 2860, 1646, 1624, 1473, 1230, 1076, 741.

Synthesis of $[Tb_4L_2(HL)_2Cl_2(\mu_3\text{-}OH)_2]Cl_2\cdot 5CH_3OH\cdot 4CH_2Cl_2$ (2). H_2L (0.15 mmol, 57 mg) was dissolved in CH_2Cl_2 (10 mL) in the presence of triethylamine (0.6 mmol, 84 μL), and then a solution of $TbCl_3\cdot 6H_2O$ (0.15 mmol, 56 mg) in absolute MeOH (3 mL) was added under stirring. The yellow solution was stirred for 12 h and then filtered. Petroleum ether was allowed to diffuse slowly into the filtrate at ambient temperature. Yellow rhombic-shaped crystals were obtained after 2 weeks. Yield: 39 mg (37%). Elem anal. Calcd for $C_{97}H_{120}Cl_{12}Tb_4N_8O_{23}$ (2827.14): C, 41.21; H, 4.28; N, 3.96. Found: C, 41.20; H, 4.23; N, 3.99. IR (KBr, cm^{-1}): 3413, 2931, 1650, 1614, 1470, 1225, 1081, 746.

Synthesis of $[Ho_4L_2(HL)_2Cl_2(\mu_3\text{-}OH)_2]Cl_2\cdot 5CH_3OH\cdot 4CH_2Cl_2$ (3). The complex was synthesized with the same procedure as that of complex **2** except $HoCl_3\cdot 6H_2O$ (0.15 mmol, 57 mg) was used instead of $TbCl_3\cdot 6H_2O$. Yield: 43 mg (40%). Elem anal. Calcd for $C_{97}H_{120}Cl_{12}Ho_4N_8O_{23}$ (2851.14): C, 40.86; H, 4.24; N, 3.93. Found: C, 40.83; H, 4.25; N, 3.91. IR (KBr, cm^{-1}): 3423, 2924, 1642, 1614, 1472, 1218, 1074, 736.

X-ray Crystallography. Suitable single crystals of complexes **1**–**3** were selected for X-ray diffraction analysis. Structural analysis was performed on an Oxford Xcalibur Gemini Ultra diffractometer using graphite-monochromated Mo Kα radiation (λ = 0.71073 Å). Data processing was accomplished with the *SAINT* processing program.[21] All data were collected at a temperature of 20 ± 2 °C. The structures were solved by direct methods, and all non-hydrogen atoms were anisotropically refined by full-matrix least squares on F^2 using the *SHELXTL-97* program.[22] The crystallographic data and structure refinement for complexes **1**–**3** are summarized in Table 1. CCDC 1024672–1024674 for **1**–**3** contain the supplementary crystallographic data for this paper. These data can be obtained free of charge from the Cambridge Crystallographic Data Centre via www.ccdc.cam.ac.uk/data_request/cif.

RESULTS AND DISCUSSION

Structural Descriptions of 1–3. X-ray crystallographic analysis reveals that all complexes **1**–**3** are isomorphically crystallized in monoclinic space group $P2_1/c$. In a typical structure of complex **1** (Figure 1a), four Dy^{III} ions are coplanar in a regular parallelogram, forming a distorted defective dicubane $\{Dy_4O_8\}$ core (Figure 1b) with three unique Dy–Dy distances of Dy1–Dy2 3.5285(6) Å, Dy1–Dy1a 3.7394(9) Å, and Dy1–Dy2a 3.8809(7) Å. In each of two equivalent $Dy_2(L)(HL)$ moieties, two Dy^{III} ions ($Dy1^{III}$ and $Dy2^{III}$ or $Dy1a^{III}$ and $Dy2a^{III}$) are linked by two μ_3-O with different coordination modes. The $Dy1^{III}$ ion is eight-coordinated by two N atoms and two phenoxy O atoms from ligand L and two μ_3-O, one phenoxy O atom, and one methoxy O atom from ligand HL, adopting a distorted bicapped triangular prism with a C_{2v} point group, while the $Dy2^{III}$ ion is nine-coordinated by two methoxy O atoms and two phenoxy O atoms from ligand L and one μ_3-O, one Cl atom, two phenoxy O atoms, and one methoxy O atom from ligand HL, forming a distorted monocapped square antiprism with a C_{4v} point group (Figure 1c). The bond distances of Dy–O are in the range of 2.294(6)–2.660(7) Å, while the bond distance of Dy–Cl is 2.682(5) Å. The bridging angles of Dy1–O9–Dy2 and Dy1–O9–Dy2a are 96.5(2) and 111.4(3)°, respectively, and the bite angles of N1–Dy1–N2, O1–Dy1–O3, O1–Dy2–O3, and O2–Dy2–O4 are 65.7(3), 70.3(2), 66.1(2), and 137.0(2)°, respectively. The selected bond lengths and angles for complexes **1**–**3** are summarized in Tables S1–S3 in the Supporting Information (SI). Notably, complexes **1**–**3** are isostructural with the reported $[Ln_4(L)_2(HL)_2(\mu_3\text{-}OH)_2Cl_2]Cl_2$ (Ln = Nd, Yb, Er, Gd)[23] and similar to $[Dy_4L_2(HL)_2(NO_3)_2(\mu_3\text{-}OH)_2]$[19d] synthesized by the same ligand. In comparison with previously reported four tetranuclear lanthanide complexes, the differences between them of the important paremeters are shown in Table 2.

Magnetic Properties. Direct-current (dc) magnetic studies were performed on polycrystalline samples of complexes **1**–**3** under an applied dc field of 100 Oe in the temperature range 1.8–300 K, as shown in Figure 2. At room temperature, for

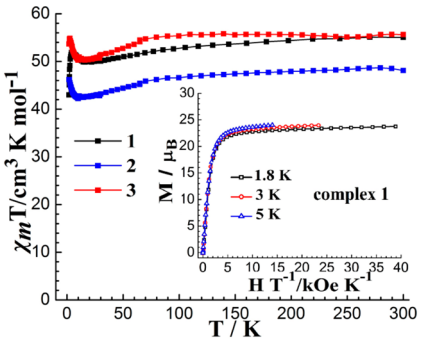

Figure 2. Temperature dependence of the $\chi_m T$ product at 100 Oe for **1**–**3**. Inset: *M* vs *H*/*T* plots for **1** at different temperatures of 1.8, 3, and 5 K.

complexes **1**–**3**, the maximum of $\chi_m T$ values are 55.06, 48.10, and 55.64 cm^3 K mol^{-1}, respectively, which are much closer to the expected values (Dy^{III}, $^6H_{15/2}$, $S = {}^5/_2$, L = 5, $g = {}^4/_3$, C = 14.17 and 56.68 cm^3 K mol^{-1}; Tb^{III}, $^7F_6$, S = 3, L = 3, $g = {}^3/_2$, C = 11.82 and 47.28 cm^3 K mol^{-1}; Ho^{III}, $^5I_8$, S = 2, L = 6, $g = {}^5/_4$, C = 14.08 and 56.28 cm^3 K mol^{-1}) for four noninteracting Ln ions.

For complex **1**, the $\chi_m T$ value undergoes a gradual reduction from 55.06 cm^3 K mol^{-1} at 300 K to 49.87 cm^3 K mol^{-1} at 16 K with decreasing temperature. While the $\chi_m T$ values increase to reach 51.88 cm^3 K mol^{-1} at 4 K before decreasing suddenly to a

DOI: 10.1021/acs.inorgchem.5b00061
Inorg. Chem. 2015, 54, 3485–3490

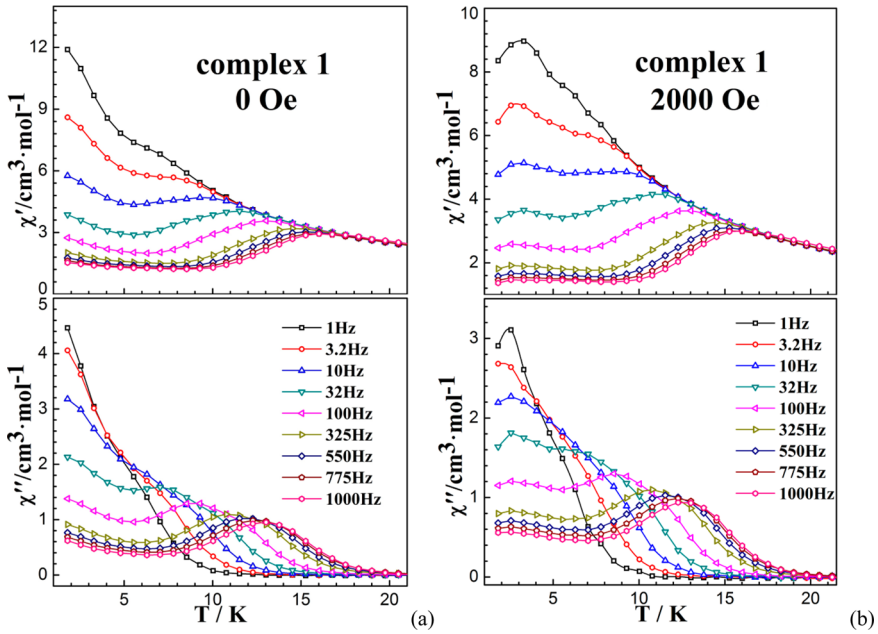

Figure 3. ac susceptibility of complex **1** under 0 (a) and 2000 Oe (b) dc field in the frequency range 1−1000 Hz.

minimum value of 42.99 cm^3 K mol^{-1} at 1.8 K. The $\chi_m T$ gradual decrease in the high-temperature range of 300−16 K is most probably governed by thermal depopulation of the Stark levels for a single Dy^{III} ion, while the $\chi_m T$ increase in the low-temperature range of 16−4 K may be due to the presence of ferromagnetic interaction between the central Dy^{III} ions. Notably, the $\chi_m T$ value decreases sharply below 4 K, which is likely attributed to Zeeman effects from the applied field, zero-field-splitting competition between ferromagnetic and antiferromagnetic coupling of Dy^{III} ions.[24] Similarly, the $\chi_m T$ value of complex **2** undergoes a gradual reduction from 48.10 cm^3 K mol^{-1} at 300 K to 45.87 cm^3 K mol^{-1} at 70 K and then decreases quickly to 42.22 cm^3 K mol^{-1} at 10 K, while the $\chi_m T$ value increases suddenly up to 46.20 cm^3 K mol^{-1} at 1.8 K. The decrease of $\chi_m T$ may be due to depopulation of the Stark levels for a single Tb^{III} ion from 300 to 70 K, and the increase from 10 to 1.8 K reveals dominant ferromagnetic interaction between the Tb^{III} center ions in the molecule.[25] The dc magnetic temperature-dependent curve of complex **3** is similar to that of complex **2**, where the maximum value of $\chi_m T$ is 55.64 cm^3 K mol^{-1} at 300 K and the value of $\chi_m T$ is 53.67 cm^3 K mol^{-1} at 1.8 K.

The field dependence of magnetization for complex **1** from 0 Oe to 70 kOe at 1.8, 3, and 5 K shows that magnetization at 1.8 K reaches the maximum of 23.75 μ_B (Figure 2, inset). The value of M in the low-H/T region becomes more rapidly saturated, indicating the ferromagnetic interactions among four Dy^{III} ions, which suggests the presence of significant magnetic anisotropy and/or low-lying excited states in complex **1**.[26] The field dependences of magnetization for complexes **2** and **3** are shown in Figures S1 and S2 in the SI, which are similar to that of complex **1**.

In order to study the magnetic relaxation dynamics of complex **1**, the alternating-current (ac) magnetic susceptibility measurements were performed as a function of the temperature and frequency on polycrystalline samples under zero and applied external dc magnetic field (Figure 3). Under zero dc field, both the in-phase (χ') and out-of-phase (χ'') signals clearly display frequency-dependent signals below approximately 20 K. As the temperature decreases from 20 to 12 K, the plot of χ'' for complex **1** gradually increases to reach a maximum of 0.95−0.29 cm^3 mol^{-1} from 1000 to 100 Hz and then decreases at even lower temperatures, which indicates that reversal of the spin has been blocked. Under an optimum dc field of 2000 Oe, two distinct peaks in the frequency range of 32 and 1000 Hz obviously perform when the quantum tunnelling of magnetization (QTM) was inhibited (Figure 3b). This proved that the two regimes of relaxation attributed to SMM behavior are controlled by two different coordination geometries of the center Dy^{III} ions (the $Dy1^{III}$ center under an eight-coordinated sphere belongs to a distorted bicapped triangular prism with a C_{2v} point group and the $Dy2^{III}$ center under a nine-coordinated sphere belongs to a distorted monocapped square antiprism with a C_{4v} point group).

Further, to probe the spin dynamics of complexes **2** and **3**, the temperature dependences of the ac magnetic susceptibilities were measured at 0 and 3000 Oe dc field, respectively. Unfortunately, no frequency-dependent signals (χ'') were observed for **2** and **3** in the absence of an applied static field. This behavior may result from the QTM commonly seen in pure multinuclear lanthanide complexes. Interestingly, complexes **2** and **3** present temperature-dependent and frequency-dependent signals of the ac susceptibility under 3000 Oe (Figures S3 and S4 in the SI), which indicate that the field-induced decoupling between the Ln ions suppresses the QTM.

The peaks of out-of-phase (χ'') signals from the frequency-dependent plots under zero dc field were used to construct the Arrhenius fitting plots (Figure 4). With the Arrhenius law $\tau = \tau_0 \exp(U_{eff}/kT)$ for complex **1**, the effective energy barrier (U_{eff}) of 55.71 K and a preexponential factor (τ_0) of 7.54×10^{-6} s afforded a linear relationship (Figure 4, bottom inset). The thermally activated behavior in the high-temperature range is mainly attributed to an Orbach relaxation process. Notably, complex **1** reveals the highest effective energy barrier (U_{eff}) among the four reported salen-type tetranuclear dysprosium SMMs, namely, $[Dy_4(\mu_3\text{-}OH)_2L_2(acac)_6]$,[19c] $[Dy_4(\mu_3\text{-}OH)_2L^2{}_2(acac)_6]$[19b] and $[Dy_4(\mu_4\text{-}O)L_2(C_6H_5COO)_6]$[17g] and $[Dy_4(salen)_6]$,[19a] respectively (Table 2). The ligand field of the

DOI: 10.1021/acs.inorgchem.5b00061
Inorg. Chem. 2015, 54, 3485−3490

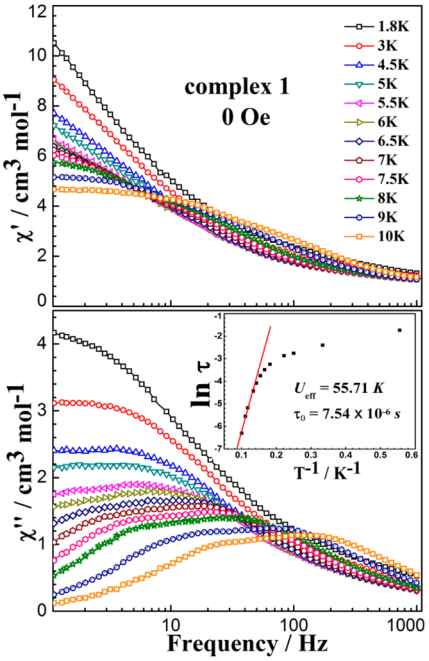

Figure 4. Plots of χ' vs frequency (top) and χ'' vs frequency (bottom) for **1** under zero dc field. Plots of ln τ vs $1/T$ for **1** (bottom inset: the red solid line represents the fitting with the Arrhenius law).

polydentate bridging ligands and the electron-withdrawing effect of the Cl counterion decrease the electron density on the Dy^{III} ions, while the electronegativities of the coordinated atoms and groups with the four reported salen-type tetranuclear dysprosium SMMs are smaller than that of complex **1**. The U_{eff} value of complex **1** is also higher than that of complex $[Dy_4L_2(HL)_2(NO_3)_2(\mu_3\text{-}OH)_2]$[19d] (48.14 K) that we used in the synthesis, which should explains why Cl atom coordination results in the lower electron density of the ligand hard plane and the larger anisotropy of Dy^{III} ions than nitrate O atom coordination of $[Dy_4L_2(HL)_2(NO_3)_2(\mu_3\text{-}OH)_2]$.

Under zero dc field, the Cole−Cole plots for complex **1** in the temprature range of 1.8−10 K (Figure 5) show the unsymmetric curves below 7.5 K, which suggest that more than one magnetic relaxation mode may exist. Using the sums of two modified Debye functions,[27] the fitting of the Cole−Cole plots gives α values in the range of 0.33−0.51 and τ values in the range of 0.0018−0.1755 (Table S4 in the SI), which suggests a relatively wide distribution of relaxation time, further indicating

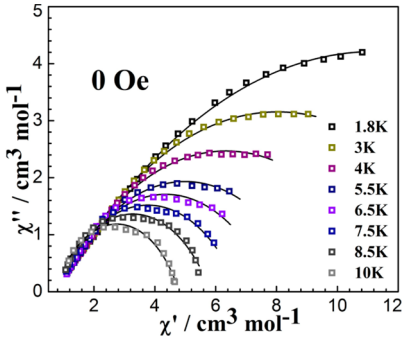

Figure 5. Cole−Cole plots for **1** obtained using the ac susceptibility data at zero dc field. The solid lines correspond to the best fit obtained with two modified Debye functions.

the presence of multiple relaxation modes. This phenomenon is similar to those of the reported polynuclear dysprosium SMMs[28] and the tetranuclear complex $[Dy_4L_2(HL)_2(NO_3)_2(\mu_3\text{-}OH)_2]$ synthesized by us. In addition, the Cole−Cole plots of $[Dy_4(salen)_6]$[19a] with two different coordination modes also present two slow relaxation processes.

CONCLUSIONS

Isolation of complexes **1**−**3** verifies that H_2L is able to react with $LnCl_3{\cdot}6H_2O$, forming a discrete tetranuclear structure with a distorted defective dicubane $\{Ln_4O_8\}$ core in which Cl ions coordinate to two crystallographically unequivalent Ln ions with C_{4v} and C_{2v} symmetry, respectively. The magnetic analysis suggests that the single-molecule magnetism for complex **1** originates from the nature of the Dy^{III} ions, while it is essentially disturbed by H_2L and Cl ions, especially the Cl ions. The two different coordination geometries with C_{4v} and C_{2v} point groups around the Dy^{III} ions result in the two relaxation dynamics for complex **1**. Strikingly, coordination of the Cl ion in terms of the electron and steric effects strengthens the magnetic anisotropy of the Dy^{III} ions, resulting in the highest energy barrier among the salen-type tetranuclear lanthanide SMMs.

ASSOCIATED CONTENT

Supporting Information

X-ray crystallographic data for complexes **1**−**3** in CIF format, additional figures of FT-IR and UV spectra, PXRD, crystal data and structure refinement, magnetic characterization for complexes **1**−**3**, selected bond lengths and angles for complexes **1**−**3**, and fitted parameters of the Cole−Cole plots for complex **1** at H_{dc} = 0 G. This material is available free of charge via the Internet at http://pubs.acs.org.

AUTHOR INFORMATION

Corresponding Author

*E-mail: gmli_2000@163.com. Tel.: 86-451-86608458.

Notes

The authors declare no competing financial interest.

ACKNOWLEDGMENTS

This work is financially supported by the National Natural Science Foundation of China (Grants 51272069, 21471051, and 51402092).

REFERENCES

(1) (a) Jenkins, M.; Huemmer, T.; Martinez-Perez, M. J.; Garcia-Ripoll, J.; Zueco, D.; Luis, F. *New J. Phys.* **2013**, 15. (b) Rinehart, J. D.; Fang, M.; Evans, W. J.; Long, J. R. *Nat. Chem.* **2011**, 538−542.

(2) (a) Bogani, L.; Maurand, R.; Marty, L.; Sangregorio, C.; Altavilla, C.; Wernsdorfer, W. *J. Mater. Chem.* **2010**, *20*, 2099−2107. (b) De Franceschi, S.; Kouwenhoven, L.; Schoenenberger, C.; Wernsdorfer, W. *Nat. Nanotechnol.* **2010**, *5*, 703−711. (c) Hong, K.; Kim, W. Y. *Angew. Chem., Int. Ed.* **2013**, *52*, 3389−3393.

(3) (a) Chen, L.; Wang, J.; Wei, J.-M.; Wernsdorfer, W.; Chen, X.-T.; Zhang, Y.-Q.; Song, Y.; Xue, Z.-L. *J. Am. Chem. Soc.* **2014**, *136*, 12213−12216. (b) Gao, F.; Cui, L.; Song, Y.; Li, Y.-Z.; Zuo, J.-L. *Inorg. Chem.* **2014**, *53*, 562−567. (c) Jia, L.-H.; Li, R.-Y.; Duan, Z.-M.; Jiang, S.-D.; Wang, B.-W.; Wang, Z.-M.; Gao, S. *Inorg. Chem.* **2011**, *50*, 144−154.

(4) (a) Boulon, M.-E.; Cucinotta, G.; Luzon, J.; Degl'Innocenti, C.; Perfetti, M.; Bernot, K.; Calvez, G.; Caneschi, A.; Sessoli, R. *Angew. Chem., Int. Ed.* **2013**, *52*, 350−354. (b) Chilton, N. F.; Langley, S. K.; Moubaraki, B.; Soncini, A.; Batten, S. R.; Murray, K. S. *Chem. Sci.*

DOI: 10.1021/acs.inorgchem.5b00061
Inorg. Chem. 2015, 54, 3485−3490

2013, *4*, 1719−1730. (c) Gao, F.; Yao, M.-X.; Li, Y.-Y.; Li, Y.-Z.; Song, Y.; Zuo, J.-L. *Inorg. Chem.* **2013**, *52*, 6407−6416. (d) Jiang, S.-D.; Liu, S.-S.; Zhou, L.-N.; Wang, B.-W.; Wang, Z.-M.; Gao, S. *Inorg. Chem.* **2012**, *51*, 3079−3087. (e) Jiang, S.-D.; Wang, B.-W.; Sun, H.-L.; Wang, Z.-M.; Gao, S. *J. Am. Chem. Soc.* **2011**, *133*, 4730−4733. (f) Song, Y.-M.; Luo, F.; Luo, M.-B.; Liao, Z.-W.; Sun, G.-M.; Tian, X.-Z.; Zhu, Y.; Yuan, Z.-J.; Liu, S.-J.; Xu, W.-Y.; Feng, X.-F. *Chem. Commun.* **2012**, *48*, 1006−1008.

(5) (a) Cao, F.; Wang, S.; Li, D.; Zeng, S.; Niu, M.; Song, Y.; Dou, J. *Inorg. Chem.* **2013**, *52*, 10747−10755. (b) Langley, S. K.; Wielechowski, D. P.; Vieru, V.; Chilton, N. F.; Moubaraki, B.; Chibotaru, L. F.; Murray, K. S. *Chem. Sci.* **2014**, *5*, 3246−3256. (c) Li, M.; Lan, Y.; Ako, A. M.; Wernsdorfer, W.; Anson, C. E.; Buth, G.; Powell, A. K.; Wang, Z.; Gao, S. *Inorg. Chem.* **2010**, *49*, 11587−11594. (d) Mishra, A.; Wernsdorfer, W.; Abboud, K. A.; Christou, G. *J. Am. Chem. Soc.* **2004**, *126*, 15648−15649.

(6) (a) Benelli, C.; Gatteschi, D. *Chem. Rev.* **2002**, *102*, 2369−2388. (b) Sorace, L.; Benelli, C.; Gatteschi, D. *Chem. Soc. Rev.* **2011**, *40*, 3092−3104.

(7) Ishikawa, N.; Sugita, M.; Ishikawa, T.; Koshihara, S.; Kaizu, Y. *J. Am. Chem. Soc.* **2003**, *125*, 8694−8695.

(8) Woodruff, D. N.; Winpenny, R. E. P.; Layfield, R. A. *Chem. Rev.* **2013**, *113*, 5110−5148.

(9) (a) AlDamen, M. A.; Clemente-Juan, J. M.; Coronado, E.; Marti-Gastaldo, C.; Gaita-Arino, A. *J. Am. Chem. Soc.* **2008**, *130*, 8874−8875. (b) Aravena, D.; Ruiz, E. *Inorg. Chem.* **2013**, *52*, 13770−13778. (c) Upadhyay, A.; Singh, S. K.; Das, C.; Mondol, R.; Langley, S. K.; Murray, K. S.; Rajaraman, G.; Shanmugam, M. *Chem. Commun.* **2014**, *50*, 8838−8841. (d) Zhang, P.; Zhang, L.; Wang, C.; Xue, S.; Lin, S.-Y.; Tang, J. *J. Am. Chem. Soc.* **2014**, *136*, 4484−4487. (e) Zhu, J.; Wang, C.; Luan, F.; Liu, T.; Yan, P.; Li, G. *Inorg. Chem.* **2014**, *53*, 8895−8901.

(10) (a) Katoh, K.; Asano, R.; Miura, A.; Horii, Y.; Morita, T.; Breedlove, B. K.; Yamashita, M. *Dalton Trans.* **2014**, *43*, 7716−7725. (b) Suzuki, K.; Sato, R.; Mizuno, N. *Chem. Sci.* **2013**, *4*, 596−600. (c) Yang, F.; Zhou, Q.; Zeng, G.; Li, G.; Gao, L.; Shi, Z.; Feng, S. *Dalton Trans.* **2014**, *43*, 1238−1245. (d) Zhang, P.; Zhang, L.; Lin, S.-Y.; Xue, S.; Tang, J. *Inorg. Chem.* **2013**, *52*, 4587−4592.

(11) (a) Andrews, P. C.; Deacon, G. B.; Frank, R.; Fraser, B. H.; Junk, P. C.; MacLellan, J. G.; Massi, M.; Moubaraki, B.; Murray, K. S.; Silberstein, M. *Eur. J. Inorg. Chem.* **2009**, 744−751. (b) Tang, J. H. I.; Madhu, N. T.; Chastanet, G.; Wernsdorfer, W.; Anson, C. E.; Benelli, C.; Sessoli, R.; Powell, A. K. *Angew. Chem., Int. Ed.* **2006**, *45*, 1729−1733. (c) Xue, S.; Zhao, L.; Guo, Y.-N.; Zhang, P.; Tang, J. *Chem. Commun.* **2012**, *48*, 8946−8948.

(12) (a) Abbas, G.; Lan, Y.; Kostakis, G. E.; Wernsdorfer, W.; Anson, C. E.; Powell, A. K. *Inorg. Chem.* **2010**, *49*, 8067−8072. (b) Chandrasekhar, V.; Das, S.; Dey, A.; Hossain, S.; Sutter, J.-P. *Inorg. Chem.* **2013**, *52*, 11956−11965. (c) Chandrasekhar, V.; Hossain, S.; Das, S.; Biswas, S.; Sutter, J.-P. *Inorg. Chem.* **2013**, *52*, 6346−6353. (d) Lin, S.-Y.; Zhao, L.; Ke, H.; Guo, Y.-N.; Tang, J.; Guo, Y.; Dou, J. *Dalton Trans.* **2012**, *41*, 3248−3252.

(13) (a) Blagg, R. J.; Muryn, C. A.; McInnes, E. J. L.; Tuna, F.; Winpenny, R. E. P. *Angew. Chem., Int. Ed.* **2011**, *50*, 6530−6533. (b) Das, S.; Hossain, S.; Dey, A.; Biswas, S.; Sutter, J.-P.; Chandrasekhar, V. *Inorg. Chem.* **2014**, *53*, 5020−5028. (c) Lin, S.-Y.; Wernsdorfer, W.; Ungur, L.; Powell, A. K.; Guo, Y.-N.; Tang, J.; Zhao, L.; Chibotaru, L. F.; Zhang, H.-J. *Angew. Chem., Int. Ed.* **2012**, *51*, 12767−12771. (d) Sharples, J. W.; Zheng, Y.-Z.; Tuna, F.; McInnes, E. J. L.; Collison, D. *Chem. Commun.* **2011**, *47*, 7650−7652.

(14) Ganivet, C. R.; Ballesteros, B.; de la Torre, G.; Clemente-Juan, J. M.; Coronado, E.; Torres, T. *Chem.—Eur. J.* **2013**, *19*, 1457−1465.

(15) (a) Alexandropoulos, D. I.; Cunha-Silva, L.; Pham, L.; Bekiari, V.; Christou, G.; Stamatatos, T. C. *Inorg. Chem.* **2014**, *53*, 3220−3229. (b) Zhang, H.; Lin, S.-Y.; Xue, S.; Wang, C.; Tang, J. *Dalton Trans.* **2014**, *43*, 6262−6268.

(16) Zhu, J.; Song, H.-F.; Yan, P.-F.; Hou, G.-F.; Li, G.-M. *CrystEngComm* **2013**, *15*, 1747−1752.

(17) (a) Habib, F.; Brunet, G.; Vieru, V.; Korobkov, I.; Chibotaru, L. F.; Murugesu, M. *J. Am. Chem. Soc.* **2013**, *135*, 13242−13245. (b) Habib, F.; Lin, P.-H.; Long, J.; Korobkov, I.; Wernsdorfer, W.; Murugesu, M. *J. Am. Chem. Soc.* **2011**, *133*, 8830−8833. (c) Habib, F.; Long, J.; Lin, P.-H.; Korobkov, I.; Ungur, L.; Wernsdorfer, W.; Chibotaru, L. F.; Murugesu, M. *Chem. Sci.* **2012**, *3*, 2158−2164. (d) Lin, P.-H.; Sun, W.-B.; Yu, M.-F.; Li, G.-M.; Yan, P.-F.; Murugesu, M. *Chem. Commun.* **2011**, *47*, 10993−10995. (e) Long, J.; Habib, F.; Lin, P.-H.; Korobkov, I.; Enright, G.; Ungur, L.; Wernsdorfer, W.; Chibotaru, L. F.; Murugesu, M. *J. Am. Chem. Soc.* **2011**, *13*, 5319−5328. (f) Wang, H.; Liu, C.; Liu, T.; Zeng, S.; Cao, W.; Ma, Q.; Duan, C.; Dou, J.; Jiang, J. *Dalton Trans.* **2013**, *42*, 15355−15360. (g) Zhang, L.; Zhang, P.; Zhao, L.; Lin, S.-Y.; Xue, S.; Tang, J.; Liu, Z. *Eur. J. Inorg. Chem.* **2013**, 1351−1357.

(18) Yang, F.; Yan, P.; Li, Q.; Chen, P.; Li, G. *Eur. J. Inorg. Chem.* **2012**, 4287−4293.

(19) (a) Koo, B. H.; Lim, K. S.; Ryu, D. W.; Lee, W. R.; Koh, E. K.; Hong, C. S. *Dalton Trans.* **2013**, *42*, 7204−7209. (b) Sun, W.-B.; Han, B.-L.; Lin, P.-H.; Li, H.-F.; Chen, P.; Tian, Y.-M.; Murugesu, M.; Yan, P.-F. *Dalton Trans.* **2013**, *42*, 13397−13403. (c) Yan, P.-F.; Lin, P.-H.; Habib, F.; Aharen, T.; Murugesu, M.; Deng, Z.-P.; Li, G.-M.; Sun, W.-B. *Inorg. Chem.* **2011**, *50*, 7059−7065. (d) Luan, F.; Yan, P.-F.; Zhu, J.; Liu, T.-Q.; Zou, X.-Y.; Li, G.-M. *Dalton Trans.* **2015**, *44*, 4046−4053.

(20) Feng, W.; Zhang, Y.; Lu, X.; Hui, Y.; Shi, G.; Zou, D.; Song, J.; Fan, D.; Wong, W.-K.; Jones, R. A. *CrystEngComm* **2012**, *14*, 3456−3463.

(21) *SMART and SAINT software package*; Siemens Analytical X-ray Instruments: Madison, WI,1996.

(22) (a) Sheldrick, G. M. *SHELXL-97, Program for X-ray Crystal Structure Refinement*; University of Göttingen: Göttingen, Germany, 1997. (b) Sheldrick, G. M. *Acta Crystallogr., Sect. B* **2008**, *64*, 112.

(23) Feng, W.; Zhang, Y.; Zhang, Z.; Lu, X.; Liu, H.; Shi, G.; Zou, D.; Song, J.; Fan, D.; Wong, W.-K.; Jones, R. A. *Inorg. Chem.* **2012**, *51*, 11377−11386.

(24) (a) Guo, Y.-N.; Chen, X.-H.; Xue, S.; Tang, J. *Inorg. Chem.* **2012**, *51*, 4035−4042. (b) Liu, J.-L.; Guo, F.-S.; Meng, Z.-S.; Zheng, Y.-Z.; Leng, J.-D.; Tong, M.-L.; Ungur, L.; Chibotaru, L. F.; Heroux, K. J.; Hendrickson, D. N. *Chem. Sci.* **2011**, *2*, 1268−1272.

(25) Mondal, K. C.; Kostakis, G. E.; Lan, Y.; Powell, A. K. *Polyhedron* **2013**, *66*, 268−273.

(26) (a) Bi, Y.; Wang, X.-T.; Liao, W.; Wang, X.; Deng, R.; Zhang, H.; Gao, S. *Inorg. Chem.* **2009**, *48*, 11743−11747. (b) Ke, H.; Zhao, L.; Guo, Y.; Tang, J. *Eur. J. Inorg. Chem.* **2011**, 4153−4156. (c) Burrow, C. E.; Burchell, T. J.; Lin, P.-H.; Habib, F.; Wernsdorfer, W.; Clerac, R.; Murugesu, M. *Inorg. Chem.* **2009**, *48*, 8051−8053.

(27) Guo, Y.-N.; Xu, G.-F.; Wernsdorfer, W.; Ungur, L.; Guo, Y.; Tang, J.; Zhang, H.-J.; Chibotaru, L. F.; Powell, A. K. *J. Am. Chem. Soc.* **2011**, *133*, 11948−11951.

(28) (a) Das, S.; Dey, A.; Biswas, S.; Colacio, E.; Chandrasekhar, V. *Inorg. Chem.* **2014**, *53*, 3417−3426. (b) Liu, C.-M.; Zhang, D.-Q.; Zhu, D.-B. *Dalton Trans.* **2013**, *42*, 14813−14818. (c) Guo, Y.-N.; Xu, G.-F.; Gamez, P.; Zhao, L.; Lin, S.-Y.; Deng, R.; Tang, J.; Zhang, H.-J. *J. Am. Chem. Soc.* **2010**, *132*, 8538−8539.

DOI: 10.1021/acs.inorgchem.5b00061
Inorg. Chem. 2015, 54, 3485−3490